MicroRNA Let-7a Down-regulates MYC and Reverts MYC-Induced Growth in Burkitt Lymphoma Cells

Valerie B. Sampson,[1] Nancy H. Rong,[1] Jian Han,[2] Qunying Yang,[2] Virginie Aris,[3] Patricia Soteropoulos,[3] Nicholas J. Petrelli,[4] Stephen P. Dunn,[1] and Leslie J. Krueger[1]

[1]Department of Molecular Genetics, Cellular and Tissue Transplantation, Alfred I. duPont Hospital for Children, Wilmington, Delaware; [2]Genaco-A Qiagen Company, Huntsville, Alabama; [3]Center for Applied Genomics, Public Health Research Institute, UMDNJ-New Jersey Medical School, International Center for Public Health, Newark, New Jersey; and [4]Helen F. Graham Cancer Center, Christiana Care Health System, Newark, Delaware

Abstract

Regulation of the MYC oncogene remains unclear. Using 10058-F4, a compound that inhibits MYC-MAX transcription factor, MYC protein and gene expression were down-regulated in Namalwa cells, a Burkitt lymphoma. Compound 10058-F4 decreased MYC mRNA (45%), MYC protein (50%), and cell growth (32%). MYC-MAX transcription factor was disrupted 24 h after treatment, resulting in transcriptional inhibition of target genes. Because microRNAs (miRNA) disrupt mRNA translation, let-7a, let-7b, and mir-98 were selected using bioinformatics for targeting MYC. Inhibition of MYC-MAX transcription factor with 10058-F4 increased levels of members of the let-7 family. In inhibited cells at 24 h, let-7a, let-7b, and mir-98 were induced 4.9-, 1.3-, and 2.4-fold, respectively, whereas mir-17-5p decreased 0.23-fold. These results were duplicated using microRNA multianalyte suspension array technology. Regulation of MYC mRNA by let-7a was confirmed by transfections with pre-let-7a. Overexpression of let-7a (190%) decreased Myc mRNA (70%) and protein (75%). Down-regulation of Myc protein and mRNA using siRNA MYC also elevated let-7a miRNA and decreased Myc gene expression. Inverse coordinate regulation of let-7a and mir-17-5p versus Myc mRNA by 10058-F4, pre-let-7a, or siRNA MYC suggested that both miRNAs are Myc-regulated. This supports previous results in lung and colon cancer where decreased levels of the let-7 family resulted in increased tumorigenicity. Here, pre-let-7a transfections led to down-regulation of expression of MYC and its target genes and antiproliferation in lymphoma cells. These findings with let-7a add to the complexity of MYC regulation and suggest that dysregulation of these miRNAs participates in the genesis and maintenance of the lymphoma phenotype in Burkitt lymphoma cells and other MYC-dysregulated cancers. [Cancer Res 2007;67(20):9762–70]

Introduction

The phenomenon of posttranscriptional gene silencing by microRNAs (miRNA) was first established in *Caenorhabditis elegans* (1). Numerous groups have identified a plethora of miRNA molecules 19 to 24 bp of noncoding, double-stranded RNA that regulate diverse sets of biological processes including cell proliferation and suppression of apoptosis (2), oncogenesis (3), viral disease (4), and hematopoietic differentiation (5). miRNAs are transcribed by RNA polymerase II initially as a primary transcript, matured by nuclease digestion, and transported into the cytoplasm as 60- to 70-bp precursors termed pre-miRNA (6). The nuclease activity generates shorter duplex RNA transcripts from pri-miRNA molecules (7). One of the double strands of the RNA duplex is highly complementary to one or more target mRNAs. Targeted mRNAs are affected by translational arrest that occurs by translational inhibition (e.g., accelerated mRNA decay or protein synthesis inhibition). This takes place on the polyribomes and, subsequently, the miRNAs are found in ribonuclear particle complexes, the RNA-induced silencing complex (8). Significant progress in deciphering the mechanism of action has been made in the area of processing of miRNA transcripts from larger precursors (6), but analogous studies with protein coding genes are expected to reveal further mechanistic and functional information about miRNA molecules.

MYC is an evolutionarily conserved nuclear protein involved in the control of cell proliferation and differentiation (9). In normal cells, MYC protein levels are transiently elevated during cell growth but decline to low levels as cells exit the cell cycle (10, 11). The MYC oncogene, first described in 1982 (12), is recognized as a key transforming oncogenic agent in a wide variety of human tumors including Burkitt lymphoma, breast and cervical carcinomas, glioblastomas, and osteosarcomas (13). The MYC protein contains a basic helix-loop-helix-leucine zipper domain (14, 15) that associates with the nuclear protein MAX to form a MYC-MAX heterodimeric transcription factor, which actively regulates the expression of various target genes involved in the control of cellular functions including apoptosis (16), and metabolism (17). Disruption of the MYC-MAX complex by mutations (14) failed to activate transcription of reporter genes. Recent studies have shown that both MYC and miRNAs influence cell proliferation and death and have identified high expression of specific miRNAs in tumor cells (18, 19).

In this study, we examined the effects of compound 10058-F4, which belongs to a class of small molecular weight compounds that inhibit MYC-MAX transcription factor by disruption of MYC-MAX heterodimers (20). We focused on real-time TaqMan relative quantitation to evaluate the potential role of miRNAs regulating the previously documented decay of Burkitt lymphoma MYC mRNAs in the presence of 10058-F4. These regulator miRNAs were also evaluated using microRNA multianalyte suspension array (mirMASA) by xMAP platform. This does not require prior amplification of the miRNAs. Time-dependent studies of the concentration of the miRNAs were also examined in parallel with determinations of the levels of MYC-MAX transcription factor and

Requests for reprints: Leslie J. Krueger, Molecular Genetics, Cellular and Tissue Transplantation, Nemours Biomedical Research, Wilmington, DE 19803. Phone: 302-651-5778; Fax: 302-651-6888; E-mail: lkrueger@nemours.org.

doi:10.1158/0008-5472.CAN-07-2462

relative levels of MYC mRNA. Finally, we examined the role of the miRNAs by transfection studies of pre-let-7a in a Myc-transfected knockout rat fibroblast line and a Myc-knockout line. Preliminary mechanistic studies of the action of the miRNAs on MYC protein and mRNA were started.

Materials and Methods

Cell lines and reagents. The B-lymphocyte cell line Namalwa was purchased from American Type Culture Collection and cultured as specified. HO15.19 MYC-knockout and MYC-transfected rat fibroblast cell lines, rat-1a-c, were a gift from Dr. Sedivy, obtained through Brown Technologies Partnership (21). Tissue culture media and supplements were obtained from Invitrogen. MYC inhibitor, compound 10058-F4 [(*Z*,*E*)-5-(4-ethylbenzylidine)-2-thioxothiazolidin-4-one], was purchased from EMD Biosciences and reconstituted and stored as previously described (22).

Treatment of cells with MYC inhibitor, compound 10058-F4. Namalwa cells (3×10^5/mL) were synchronized by serum starvation in RPMI 1640 supplemented with 0.5% fetal bovine serum (FBS) for 48 h. Cells were stimulated to reenter the cell cycle using RPMI 1640 supplemented with 10% FBS. Compound 10058-F4 was added to the cells to final concentrations of 60, 90, and 120 μmol/L. For each concentration of compound, cells were harvested at 24-, 48-, and 72-h intervals. Control cells were also harvested at the same time intervals in the absence of compound.

RNA preparation and concentration determination. Total RNA was isolated after cells were harvested using the mirVana miRNA Isolation Kit purchased from Ambion according to the manufacturer's instructions. RNA concentration was measured using the Quant-iT RiboGreen RNA Assay Kit from Molecular Probes. The purity of the RNA was analyzed using 1 μL of total RNA on a nanoRNA LabChip using the Agilent 2100 bioanalyzer from Agilent.

Reverse transcription and quantitative real-time PCR. Reverse transcription for miRNAs was done using total RNA and the High-Capacity cDNA kit, the TaqMan MicroRNA Assays Human Panel, and miRNA-specific reverse transcription primers, which were all supplied by Applied Biosystems. Reverse transcription was done according to the manufacturer's protocol. First-strand cDNA was also generated from total RNA using the High-Capacity cDNA kit. Quantitative PCR was done for both miRNA and gene expression assays on an ABI PRISM 7600 DNA Sequence Detection System from Applied Biosystems. The "comparative threshold" method was used to calculate relative gene expression. Values were normalized against mir-141 for miRNAs and 18S rRNA for MYC and MYC target genes.

miRNA measurements using mirMASA technology. Total RNA (15–20 μg) isolated from cells incubated with or without 60 μmol/L of MYC compound for 24, 48, and 72 h was analyzed using the mirMASA, which uses locked nucleic acids to stabilize hybridization and allow direct capture of miRNAs in a multiplex reaction designed by GENACO-A Qiagen Company.[5]

3-(4,5-Dimethylthiazol-2-yl)-2,5-diphenyltetrazolium bromide cell proliferation assay. Namalwa cells were seeded on a 96-well plate at a density of 3×10^5/mL and treated with 60 μmol/L of compound. Cell viability was determined by incorporation of 3-(4,5-dimethylthiazol-2-yl)-2,5-diphenyltetrazolium bromide (MTT) as previously described (22).

Cell death detection. Namalwa cells (4×10^4) were either untreated or treated with 60 μmol/L of compound 10058-F4 for 24, 48, and 72 h. Analysis of DNA fragmentation was done using the Cell Death Detection ELISA Kit (Roche) according to the manufacturer's instruction. Cell death was measured by the ELISA assay using an ELISA plate reader at λ = 405 nm and λ_{ref} = 490 nm.

Immunoprecipitation of MYC-MAX complexes. Cells grown with or without treatment with 60 μmol/L of MYC compound were harvested at 24 and 48 h. Cytoplasmic and nuclear fractions were prepared using the Nuclear Extraction Kit according to the manufacturer's protocol (Imgenex). Protein concentrations were measured by the Bio-Rad protein assay. Approximately 400 μg of protein from each cell extract were precleared by rocking for 1 h with protein G-agarose beads (Santa Cruz Biotechnology) and centrifuged at 1,000 × *g* for 5 min. Supernatants were incubated with polyclonal anti-MYC antibody (Santa Cruz Biotechnology) for 4 h at 4°C. Control experiments were done with normal rabbit immunoglobulin G (IgG). Fifty microliters of protein-G beads in PBS buffer were added and incubated overnight. The beads were precipitated at 1,000 × *g* for 5 min and washed thrice with PBS buffer. Fifty microliters of 4× SDS-PAGE sample buffer were added and immunoprecipitates denatured by heating to 100°C for 5 min.

Western blot analysis. Cytoplasmic and nuclear cell fractions and MYC immunoprecipitates were resolved on a 10% SDS/PAGE gel and transferred onto a polyvinylidene difluoride membrane purchased from Bio-Rad. The membrane was blocked with 5% nonfat dry milk in TBS containing 0.1% Tween 20 at room temperature for 1 h and incubated with either monoclonal anti-MYC antibody or monoclonal MAX antibody (Santa Cruz Biotechnology) overnight at 4°C, followed by incubation with the secondary antibody horseradish peroxidase–conjugated donkey anti-mouse IgG (Santa Cruz Biotechnology). Proteins were detected using Supersignal Western Pico Chemiluminescent Substrate (Pierce). Loading control was determined with anti-actin antibody purchased from Sigma.

Tranfections of rat fibroblasts. Myc-transformed rat fibroblasts 1a-c were transfected into six-well plates at a cell density of 2.3×10^5 per well. Transfections were done using the siPORT NeoFX (Ambion) transfection reagent according to the manufacturer's protocol, with a final concentration of 40 nmol/L of MYC-specific siRNA, negative control siRNA, let 7a-1 precursor miRNA, or control miRNA. After 48 h of transfection, cell lysates were harvested and assayed by Western blotting or quantitative real-time reverse transcription-PCR (RT-PCR) as described above.

Results

MYC mRNA expression levels and cell growth in cells treated with MYC inhibitor. Previous studies in our laboratory showed that compound 10058-F4 reduced MYC mRNA expression levels in a B-lymphoblastoid and two other Burkitt lymphoma cell lines (22). Here, an additional Burkitt lymphoma cell line, Namalwa, was studied. These cells were initially established from an endogenous Burkitt lymphoma and have two copies of the EBV integrated in a head-to-tail orientation (23). Namalwa does not contain episomal EBV and the characteristic t(8:14) activates MYC (10). Using this extensively characterized line, we systematically investigated the mechanism of the decline of MYC mRNA. First, the effects of various concentrations of compound 10058-F4 (60, 90, and 120 μmol/L) on MYC mRNA levels were measured in logarithmically growing cultures (seeded at 3×10^5 cells/mL). Aliquots of each culture were sampled after 48 h, total RNA was prepared as described (Materials and Methods), and MYC mRNA levels were measured by real-time RT-PCR. In agreement with previous findings (22), MYC mRNA expression was found to be dose dependent as shown in Fig. 1*A*. The average expression of the MYC mRNA decreased to 70%, 44%, and 37% of control cells in the presence of 60, 90, and 120 μmol/L of compound, respectively. Using 60 μmol/L of compound 10058-F4, a time-related response curve of MYC mRNA was measured at 24-h intervals. In this dynamic analysis of the effects of the compound on MYC mRNA, it was noted that at 24 h, the relative amounts of MYC mRNA were similar to control levels, but at 48 and 72 h, decreased by 37% and 45%, respectively (Fig. 1*B*). These results confirmed similar results obtained in previous studies (22) where MYC mRNA levels were down-regulated in a dose-dependent and time-related manner. From the above data, we selected a compound

[5] http://gene.genaco.com/technology.html

concentration of 60 μmol/L and time course of 48 h that is specific to Namalwa cells.

Correlative studies of cellular parameters were also carried out, including cell growth and viability. Analysis of growth was done both by direct cell count using trypan blue exclusion for viability and by the MTT assay. For cultures initiated at 3×10^5 cells/mL and exposed to 60 μmol/L of compound, the resultant growth curve showed an average decrease of cell numbers by 7.5%, 24.4%, and 32% at 24, 48, and 72 h, respectively, as determined by direct cell counts (Fig. 1*C*). Cells exposed to 60 μmol/L of compound were analyzed as well by the MTT assay and showed a decrease in absorbance by 4.9% and 20.7% at 24 and 48 h (Fig. 1*D*). The most significant change was observed at 72 h with a 42.5% decrease in absorbance. These current results confirm the antiproliferative effect of the compound on cell number as well as mitochondrial metabolic activity first reported in ref. 22. Additionally, the cells undergoing apoptosis were measured by an ELISA assay, which showed <10% apoptotic cells over the time course of treatment with compound 10058-F4 (data not shown).

Compound-induced decreases in the levels of MYC-MAX transcription factor affect MYC mRNA levels. Although the half-lives of both MYC mRNA and protein are extremely short (24), we examined the association between the compound-induced declines. Namalwa cells were exposed to 60 μmol/L of 10058-F4 compound and timed aliquots (24 and 48 h) were removed for nuclear and cytoplasmic isolation. Lysates were subjected to immunoprecipitations with anti-MYC antibody, and MYC-MAX transcription factor was determined by Western blot analysis for the levels of MAX contained in the initial immunoprecipitation as follows: MYC was immunoprecipitated from 400 μg of total protein from cytoplasmic and nuclear extracts of Namalwa cells that were exposed to 10058-F4 for 24 h. The extracts were immunoblotted with anti-MYC and anti-MAX antibodies, which showed bands at the appropriate molecular weights, 62-kDa for MYC (Fig. 2*A*) and

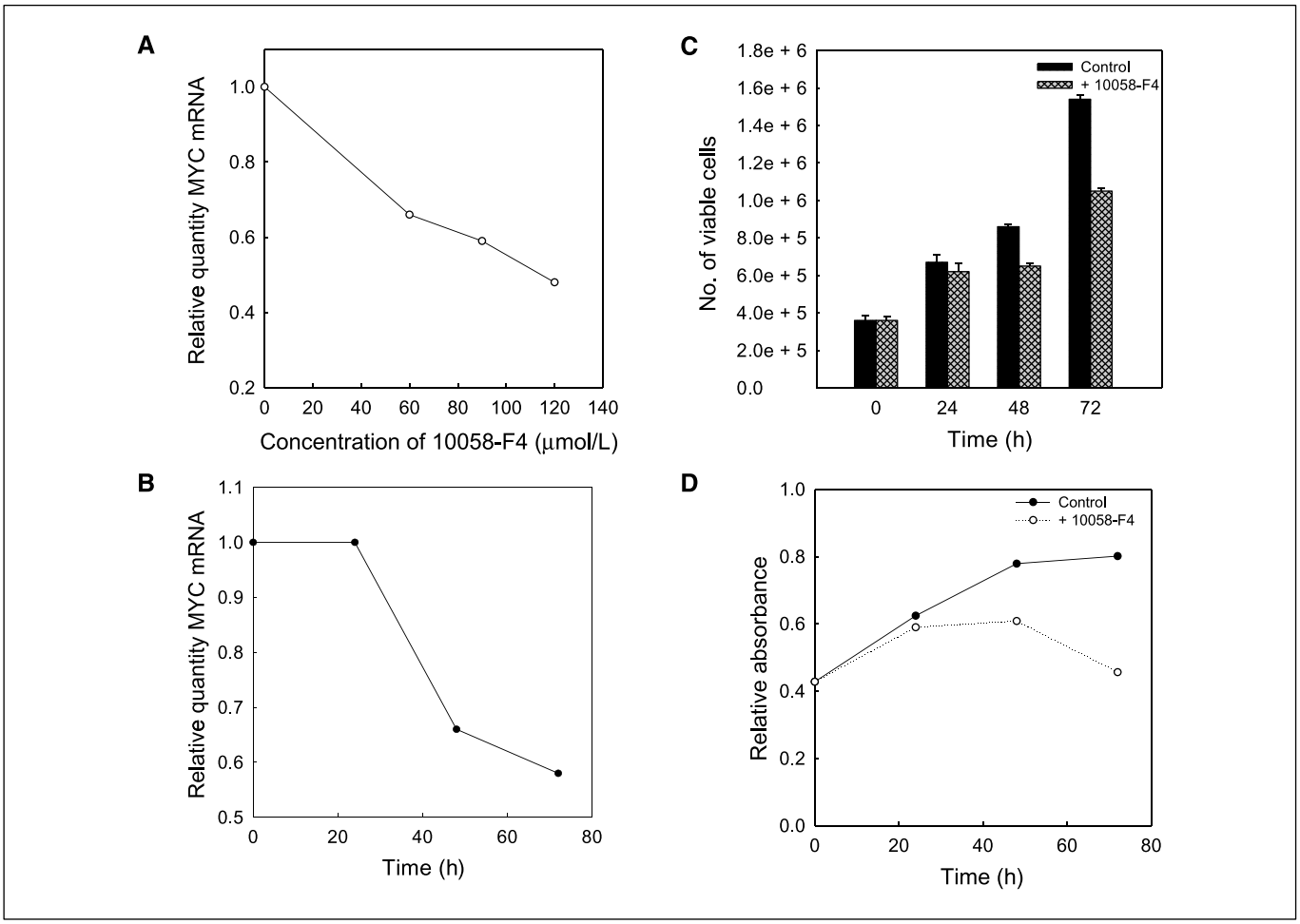

Figure 1. Effects of 10058-F4 on the levels of MYC mRNA and on the growth of Namalwa Burkitt lymphoma cells. *A,* 10058-F4 concentration dependency of MYC mRNA levels. Cells seeded at a density of 3×10^5/mL were serum starved and then fed with complete medium containing 60, 90, or 120 μmol/L of 10058-F4 for 48 h. Cells were harvested and total RNA was extracted. MYC mRNA was measured by real-time TaqMan RT-PCR using the MYC gene expression assay with 18S rRNA as endogenous control. Relative quantity was calculated using the comparative threshold method. *Points,* average of quadruplicate PCR reactions. *B,* 10058-F4 time dependency of MYC mRNA levels. Cells (see above) were treated with 60 μmol/L 10058-F4; harvested at 0, 24, 48, and 72 h; and MYC mRNA levels were calculated (see above). *Points,* average of quadruplicate PCR reactions. *C,* cell growth studies in the presence and absence of 60 μmol/L 10058-F4. Namalwa cells exposed to 60 μmol/L compound and controls were aliquoted for viable cell counts at 0, 24, 48, and 72 h. *Solid columns,* counts for untreated cells; *checkered columns,* counts for treated cells. *Columns,* mean for triplicate cell counts; *bars,* SE. *D,* cell proliferation analysis with the MTT assay. Cells were grown in a 96-well plate and incubated with 10058-F4 (60 μmol/L) for the indicated times. Time-dependent changes in cell number were determined by the MTT assay (Materials and Methods). The absorbance (562 nm) of cells treated with compound (○) was plotted against untreated control cells (●). *Points,* mean for replicates of six wells.

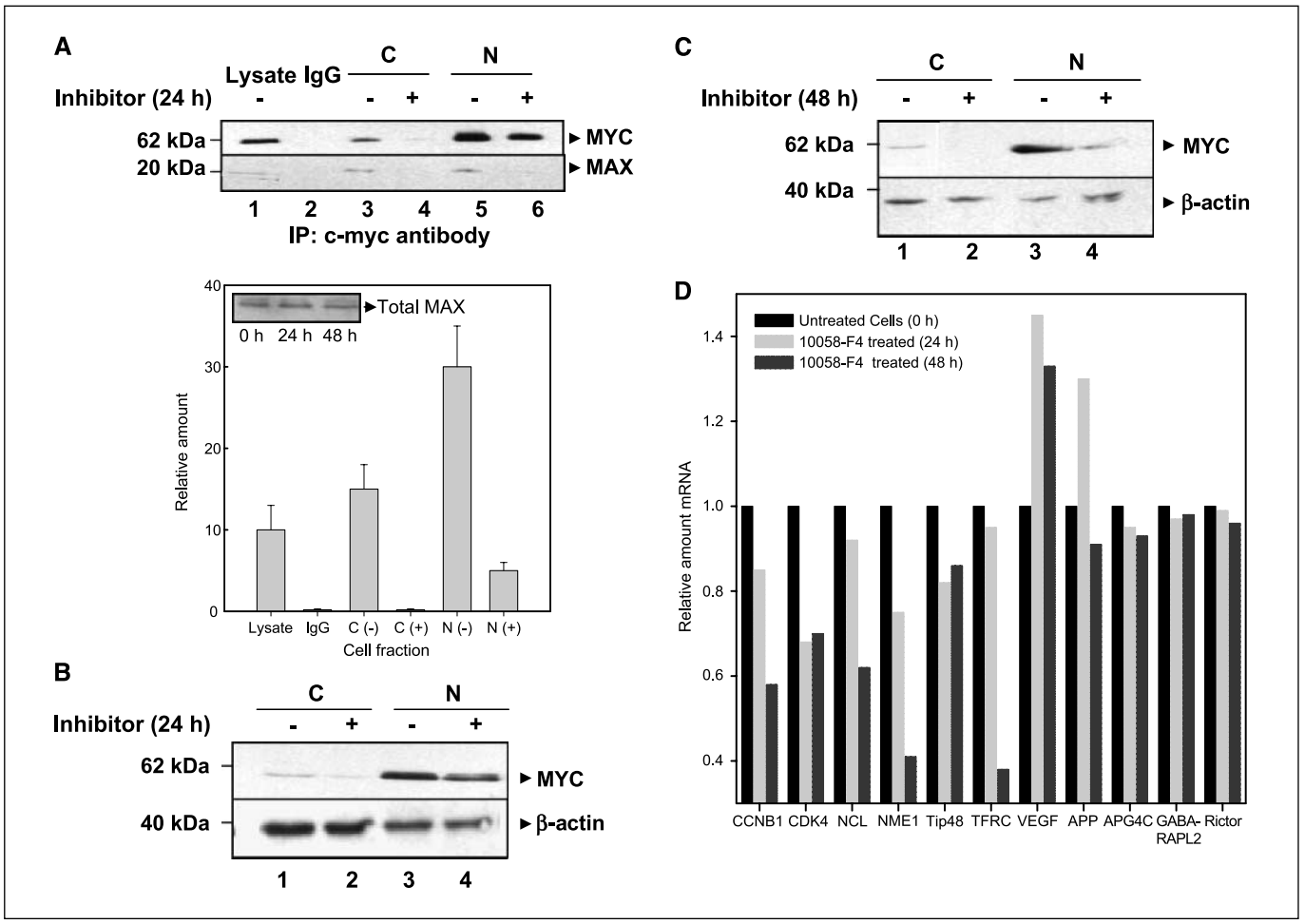

Figure 2. Effect of compound 10058-F4 on MYC and MAX protein concentrations and MYC target genes. *A,* detection of levels of MYC-MAX transcription factor (*TF*) complexes by immunoprecipitation with anti-MYC and subsequent immunoblotting and quantification with anti-MAX. MYC immunoprecipitates obtained from cytoplasmic (*C*) and nuclear (*N*) extracts of cells treated with 10058-F4 for 24 h were immunoblotted with anti-MYC and anti-MAX antibodies (*top*). At 24 h, the densitometric results of the anti-MAX immunoblots for the lysate, control, cytoplasmic (+/− compound), and nuclear (+/− compound) anti-MYC immunoprecipitates were plotted (*bottom*). *Columns,* average amount of MYC-MAX complexes in compound-treated versus untreated cytoplasmic and nuclear extracts from three independent experiments; *bars,* SE. The amount of MAX determined by immunoblotting over time is shown for the initial lysates at 0, 24, and 48 h (*bottom, inset*). *B,* detection of MYC protein levels in 24-h exposed Namalwa cells. Cytoplasmic and nuclear fractions extracted from Namalwa cells with (+) or without (−) treatment by 60 μmol/L 10058-F4 for 24 h were subjected to Western blot analysis with MYC antibodies. β-Actin was analyzed as a control. *C,* detection of MYC protein levels in 48-h exposed Namalwa cells. Immunoblot for MYC and β-actin after 48-h compound exposure was done as described in *C. D,* effects of 10054-F4 exposure on MYC target genes. MYC-MAX transcription factor–activated and MYC-MAX transcription factor–repressed genes, as well as controls, were evaluated for changes in mRNA levels by real-time TaqMan RT-PCR relative quantification. *Black columns,* untreated control cells; *light gray* and *dark gray columns,* 24 and 48 h of treatment for each target mRNA. *Columns,* average of quadruplicate PCR reactions.

20-kDa for MAX (Fig. 2*A*). Nuclear fraction lysates that were exposed to the compound showed a 5-fold decrease in MYC-MAX transcription factor. MAX protein levels assayed in total cell lysates at 0, 24, and 48 h after drug exposure showed no change in the concentrations over time (Fig. 2*A, bottom, inset*) although the decrease in the MYC-MAX transcription factor (as measured above) was maintained for at least 48 h (data not shown).

We also examined the effects of the compound on the levels of total MYC protein. Overall, the monoclonal antibodies directed against MYC detected the 62-kDa MYC protein predominately present in the nucleus (Fig. 2*B*). Densitometric analysis (data not shown; $n = 3$) indicated the loss of MYC protein was ~3-fold in both the cytoplasmic and nuclear fractions after 24 h. MYC protein expression was further reduced by 10-fold in the nuclear fraction after 48 h of compound exposure ($n = 3$; Fig. 2*C*). β-Actin expression was unchanged in all experimental and control points.

Changes in the expression of MYC target genes correlate to MYC-MAX transcription factor inhibition. MYC-MAX transcription factor–dependent regulation of numerous target genes has previously been studied (13, 25).[6] The extent of target gene regulation by MYC-MAX transcription factor is dependent on the affinity for genomic binding sites and levels of the transcription factor (26). Quantitative real-time PCR assays were used to measure relative expression levels of a select subset of previously identified MYC-MAX transcription factor target and nontarget genes (Fig. 2*D*). Nine of these are MYC-MAX transcription factor regulated by MYC and are categorized in the Gene Ontology database as cell cycle (*CCNB1, CDK4*), biosynthesis (*NCL1*), gene

[6] http://www.myc-cancer-gene.org/site/mycTargetDB.asp

expression (*NME1, Tip48*), metabolism (*TFRC, GAPD*), and growth (*VEGF, APP*). The observed changes were specifically altered in appropriate ways by MYC-MAX transcription factor inactivation. *APG-1, APG4C, GABARAPL2*, and *Rictor* were regulated independently from MYC-MAX transcription factor changes and the PCR results for these genes were unaffected by the compound (Fig. 2*D*).

Overexpression of miRNAs in cells exposed to MYC inhibitor. Because miRNAs target mRNA for either degradation or translational inhibition, and because mRNA degradation was documented for MYC RNA in Namalwa cells (see above) and three other cell lines (22), the miRNA levels specific to MYC mRNA were measured. Our initial database search at the http://www.microrna.org website identified mir-34b, mir-98, let-7a, let-7b, let-7c, and let-7f as miRNAs potentially targeting MYC mRNA. The bioinformatic targets[7] of these miRNAs were then crossed-referenced with the MYC oncogene database[8] to determine the relationship between miRNAs and their potential targets. The result was then graphed using cytoscape[9] to show the interactions between MYC-associated miRNAs and their potential mRNA targets. The nodal nature of the targets and their overlaps suggests that MYC-associated miRNAs work in concert (Fig. 3*A*; Table 2). Using total extracted RNA from cells with or without exposure to 60 μmol/L of 10058-F4 for 48 h, a quantitative real-time PCR analysis of miRNA human panel was done, which showed that of the six putative miRNAs targeting MYC mRNAs, let-7a and let-7b of the let-7 cluster were distinctly overexpressed by 1.6- and 1.73-fold, respectively. mir-98 was increased by 2.1-fold in compound-exposed cells relative to control (Table 1). The changes in expression levels of let-7c and let-7f were not significantly different from controls (data not shown). The mir-34b primers were not present in the panel. Relative expression levels were normalized against mir-141.

We validated these results (Table 1) and extended them to determining the time-dependent profiles of these miRNAs in cells exposed to compound for 24, 48, and 72 h using mirMASA technology. This locked nucleic acid–based technology that measures miRNA amounts directly confirmed our PCR data. The expression profile of let-7a corresponded to a 4.9-fold increase at 24 h and a 2-fold increase at 48 and 72 h (Fig. 3*B*). A similar pattern was obtained for mir-98 (Fig. 3*B*), which showed 2.5-, 1.8-, and 1.2 fold increases at 24, 48, and 72 h, respectively, over control amounts. There was a 1.2-fold increase in let-7b expression levels at 24 h (Fig. 3*B*), but a decrease at 48 and 72 h below controls. Because it was previously shown that expression of the mir-17 cluster was induced by MYC (3, 27), we measured the expression profile of mir-17-5p. The results showed that mir-17-5p was reduced 0.23-, 0.02-, and 0.27-fold at 24, 48, and 72 h, respectively. The overall down-regulation of mir-17-5p on MYC inhibition observed here strongly supports the previously reported up-regulation in cells that express high levels of MYC (27). Taken together, these results show distinct time-dependent changes in expression profiles for let-7a, let-7b, mir-98, and mir-17-5p in the presence of compound 10058-F4. Of note, the most significant changes occurred early, within a period of 24 h of compound treatment.

A classic washout experiment was done to determine whether the RNA changes were caused by the effect of compound 10058-F4. Cells previously exposed to 60 μmol/L of compound for 48 h were harvested by centrifugation and regrown in complete RPMI 1640 without compound for an additional 48 h. These cells showed renewed growth when transferred to compound-free medium (data not shown). Expression levels of mRNA and miRNA were also measured. In the first 48 h of compound treatment, relative expression levels of let-7a, let-7b, and mir-98 were up-regulated as previously described (Table 1). Within 48 h after compound removal, the amounts of let-7a, let-7b, and mir-98 were reduced by 32%, 18%, and 53%, respectively (Fig. 3*C*). MYC transcript levels increased by 55% on removal of the compound (Fig. 3*C*). These results verified that the observed global changes in let-7a, let-7b, mir-98, and MYC mRNA (Fig. 2*A* and *B*) were both drug induced and reversible.

***In vitro* gene silencing of Myc mRNA by siRNA MYC and pre-let-7a.** The mechanism for the apparent miRNA-mediated decrease in Myc mRNA was investigated by transient transfection of pre-let-7a molecules. In using the immortalized rat HO15.19 fibroblasts, a homozygous knockout of Myc and its paralogues (21), as well as the Myc-transfected derivative line rat 1a-c-Myc, we found that transfection of 2.3×10^5 rat 1a-c-Myc cells with pre-let-7a resulted in an increase at 48 h posttransfection of let-7a miRNA and a concomitant decrease in Myc mRNA (Table 2). Duplicate cultures were harvested for the analysis of Myc protein by Western blot and densitometry. Scanning of the resultant autoradiography indicated that the protein was decreased by 25% (Fig. 4*A, lane 5*). In a parallel transfection experiment, the effects of siRNA MYC as well as the effect of 60 μmol/L compound 10058-F4 resulted in similar regulation of let-7a and Myc mRNA (Table 2), whereas Myc protein was decreased ~50% (Fig. 4*A, lanes 3* and *4*). As expected, Myc mRNA and protein were undetectable in rat HO15.19 fibroblasts, the Myc-knockout cells.

The rat knockout, siRNA MYC–transfected, 10058-F4–treated, and pre-let-7a–transfected fibroblasts showed 7.1-, 2.1-, 4.4-, and 1.9-fold increases in expression levels of let-7a and 0.0-, 0.4-, 0.9-, and 0.3-fold less Myc mRNA, respectively, when compared with rat 1a-c Myc-transformed cells (Table 2). Further, the rat knockout, siRNA Myc–transfected, 10058-F4–treated, and pre-let-7a–transformed fibroblasts showed 0.6-, 0.8-, 0.7-, and 0.3-fold decreases of mir-17-5p compared with rat 1a-c Myc-transformed cells. Using rat 1a-c-Myc miRNA levels as calibrator for real-time PCR, the ratio of the miRNA levels for let-7a and mir-17-5p in the siRNA MYC– or pre-let-7a–transformed cells, as well as in 10058-F4–exposed cells, were plotted against Myc mRNA expression levels. Although the slopes of the two miRNA were opposite with let-7a (positive) and mir-17-5p (negative), their ratio, when plotted against Myc mRNA levels, formed a straight line, with $r^2 = 0.99$ (Fig. 4*B*).

Discussion

Johnson et al. (28) first described the suppression of RAS by let-7a by showing that let-7 expression is down-regulated in lung tumors more than in normal lung tissue, resulting in RAS protein levels being significantly higher in tumors. This relationship has been confirmed in colon cancer where it seemed that MYC was also down-regulated by let-7 (29). The rat fibroblast line HO15.19 containing a homozygous deletion of endogenous Myc and its paralogues (a genetically engineered Myc null cell line) and the same line but containing a promoter-enhanced wild-type Myc,

[7] Obtained from www.microrna.org.
[8] http://www.myc-cancer-gene.org/site/mycTargetDB.asp
[9] http://www.cytoscape.org

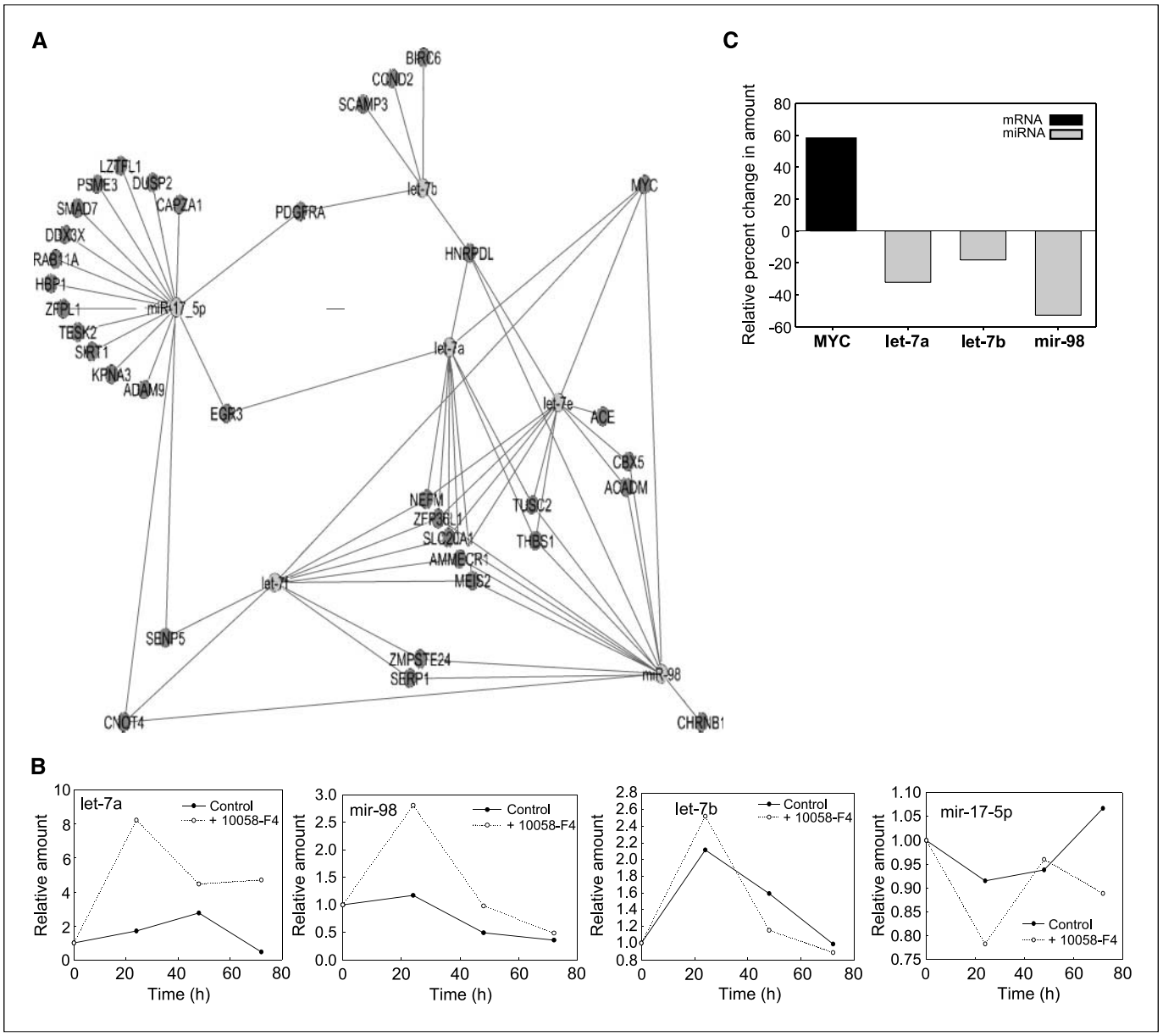

Figure 3. Expression profiles of miRNAs and MYC mRNA. Direct determination of miRNA levels in exposed cells. *A,* the list of potential targets of the MYC-associated miRNAs (see above) was cross-referenced with the list of known MYC-MAX transcription factor downstream regulated genes.[9] The resultant graph is shown indicating the overlaps and interrelationships of the MYC-associated miRNA target list. *B,* Namalwa cells treated with or without 60 μmol/L 10058-F4 were harvested at 0, 24, 48, and 72 h. Total RNA (15–20 μg) isolated was used to determine the expression levels of let-7a, mir-98, let-7b, and mir-17-5p using mirMASA at the indicated times. Each value was normalized to 5S rRNA. Relative amounts of miRNA in cells treated with compound (○) were plotted against untreated control cells (●). Relative changes in MYC mRNA and miRNA expression levels on removal of inhibition. Cells exposed to 60 μmol/L 10058-F4 for 48 h were further grown in RPMI 1640 without compound for 48 h and total RNA was extracted. MYC mRNA and let-7a, let-7b, and mir-98 levels were measured by real-time TaqMan RT-PCR (see Materials and Methods). *C,* relative percent changes in the amounts of mRNA and miRNAs measured after compound removal.

rat-1a-c (21) were initially used to confirm the specificity and nontoxicity of the MYC inhibitor 10058-F4 (22). Here, by transfection experiments, the results confirmed (29) and extended to Burkitt lymphoma the linkage between Myc and let-7a miRNA concentrations (Table 2). Transient transfections of all reagents used (pre-let-7a and siRNA MYC) or exposure to 10058-F4 resulted in the down-regulation of MYC mRNA. Coupled to this MYC down-regulation, the concentrations of miRNA let-7a (range, 1.0–4.4) and mir-17-5p (0.3–1.0) were markedly changed, but in opposite directions. In every case tested, a nonstoichiometric and inverse relationship between MYC mRNA and let-7a was found. A 29% reduction in MYC expression of control cells as compared with HO15.19-MYC cells transfected with MYC siRNA resulted in the doubling of let-7a whereas mir-17-5p levels were decreased, as measured by real-time PCR (Table 2). Consistent with these reciprocal findings, in the absence of MYC in the HO15.19 knockout cell line, the endogenous mir-17-5p levels were substantially lower than all the treatments with the exception of the inhibitor-treated cells. This confirmed the expected MYC-MAX transcription factor up-regulation of mir-17-5p (27). O'Donnell et al. (27) first described the presence of MYC-binding sites contained within the C13orf25, which include mir-17-5p. Evaluating several highly evolutionarily

conserved sequences between mouse and man, they showed binding of MYC to canonical and noncanonical MYC recognition sequences. In opposition, in the absence of MYC, let-7a miRNA concentration was the highest of all experimental procedures tested including transfection of siRNA MYC into HO15.19-MYC or the precursor to let-7a (see Table 2). This apparent coordinate relationship between the two miRNAs was supported by the results of plotting the relative ratios of the two miRNAs versus the effects MYC mRNA concentration for each experimental agent (r^2 = 0.99) as shown in Fig. 4*B*. Thus, miRNA-MYC mRNA form an autoloop in an inverse and reciprocal manner. These types of autoregulator loops are becoming more common as more miRNA-target complexes are defined (27, 30). Subsequently, several groups (31, 32) have shown the autoloop nature of the regulation of mir-17-5p, MYC, and the E2F* family of transcription factors. The regulation of translation of E2F1 protein by mir-17-5p was documented (31) in breast cancer cells and then rapidly confirmed in prostrate and hematologic malignancies (32, 33). These previous studies confirmed a similar kind of miRNA-mRNA regulation that is being suggested here. In summary, despite the varying efficiencies of the individual agents used to target MYC-MAX transcription factor regulation, the ratio of the two miRNAs remained the same although the slope of mir-17-5p was positive and let-7a was negative. Additionally, we showed an inverse and reciprocal relationship between MYC mRNA and let-7a levels (Table 2). We also examined whether these regulatory changes remained fixed in the cell. In the 10058-F4 washout experiment, the opposite results were obtained where the MYC mRNA concentrations returned to near normal (Fig. 3*C*) whereas the let-7a level declined. Again, these results reinforce a direct relationship between MYC-MAX transcription factor concentrations (Fig. 2*A, bottom*) and let-7a levels.

Previously, we showed that exposing a single lymphoblastoid or two Burkitt lymphoma cell lines to the MYC inhibitor caused a decrease in their cancerous consequence. While documenting the antiproliferative effects of 10058-F4, we discovered the unprecedented and unilateral decay of MYC mRNA (22) in the presence of a molecule that disassociated and disrupted the MYC-MAX transcription factor. Whereas the observation of the mRNA decline has now been well documented (Fig. 1*A* and *B*; ref. 22), the

Table 1. Differential expression of miRNAs and their MYC-associated target genes

MYC-targeting miRNAs			Potential downstream miRNA targets overlapping MYC-regulated genes		
miRNA	Potential target gene	Fold change in the presence of 10058-F4 for 48 h	Gene symbol	UniGene ID	Gene title
let-7a	MYC	1.6	*AMMECR1*	Hs.481208	Alport syndrome
			EGR3	Hs.534313	Early growth response 3
			HNRPDL	Hs.527105	Heterogeneous nuclear ribonucleoprotein D-like
			MEIS1	Hs.510989	Meis1, myeloid ecotropic viral integration site 1 homologue 2
			MYC	Hs.202453	V-myc myelocytomatosis viral oncogene homologue (avian)
			NEFM	Hs. 458657	Neurofilament, medium polypeptide 150 kDa
			SLC20A1	Hs.187946	Solute carrier family 20 (phosphate transporter), member 1
			THBS1	Hs. 164226	Thrombospondin 1
			TUSC2	Hs.517981	Tumor suppressor candidate 2
			ZFP36L1	Hs.85155	Zinc finger protein 36, C3H type-like 1
let-7b	MYC	1.73	*BIRC6*	Hs. 150107	Baculoviral IAP repeat-containing 6 (apollon)
			CCND2	Hs.376071	Cyclin D2
			HNRPDL	Hs.527105	Heterogeneous nuclear ribonucleoprotein D-like
			PDGFRA	Hs.74615	Platelet-derived growth factor receptor, α polypeptide
			SCAMP3	Hs.200600	Secretory carrier membrane protein 3
miR-98	MYC	2.1	*ACADM*	Hs.445040	Acyl-CoA dehydrogenase
			AMMECR1	Hs.481208	Alport syndrome
			CBX5	Hs.632724	Chromobox homologue 5 (HP1α homologue, *Drosophila*)
			CHRNB1	Hs.330386	Cholinergic receptor, nicotinic, β1 (muscle)
			CNOT4	Hs. 490224	CCR4-NOT transcription complex, subunit 4
			HNRPDL	Hs.527105	Heterogeneous nuclear ribonucleoprotein D-like
			MEIS1	Hs.510989	Meis1, myeloid ecotropic viral integration site 1 homologue 2
			MYC	Hs.202453	V-myc myelocytomatosis viral oncogene homologue (avian)
			SERP1	Hs.518326	Stress-associated endoplasmic reticulum protein 1
			SLC20A1	Hs.187946	Solute carrier family 20 (phosphate transporter), member 1
			THBS1	Hs.164226	Thrombospondin 1
			TUSC2	Hs.517981	Tumor suppressor candidate 2
			ZFP36L1	Hs.85155	Zinc finger protein 36, C3Htype-like 1
			ZMPSTE24	Hs.591501	Zinc metallopeptidase (STE24 homologue, yeast)
mir-141	Calibrator	1.0			

NOTE: MYC-associated target genes were determined by finding the union of MYC-regulated genes and the list of potential miRNA target genes.

Table 2. Differential expression of Myc mRNA and miRNAs let-7a and mir-17-5p in rat-1a-c Myc-transformed fibroblast cells treated with siRNA MYC, pre-let-7a, and 60 μmol/L of compound 10058-F4 for 72 h compared with untreated HO15.19 Myc-knockout cells

Treatment	Relative amount of Myc mRNA	Relative amount of let-7a	Relative amount of mir-17-5p
Untreated rat-1a-c cells	1.0	1.0	1.0
siRNA MYC (rat-1a-c)	0.6	2.1	0.8
pre-let-7a (rat-1a-c)	0.7	1.9	0.7
10058-F4 (rat-1a-c)	0.1	4.4	0.3
Untreated HO15.19 cells	0.0	7.1	0.4

mechanism of action still remains unknown. Therefore, we planned a series of experiments to investigate the mechanism of this unique finding. Because miRNAs were known to inhibit protein synthesis by several mechanisms (as recently reviewed in refs. 34, 35) including mRNA decay, we decided to determine the temporal relationship between candidate miRNAs that might regulate MYC mRNA. As one of the first documented cases of regulation (other than let-7 or lin-4 in *Arabidopsis*) was the specific cleavage of the mRNAs encoding several of the Scarecrow-like family of putative transcription factors by mir-171 (36), there already was a precedent for this examination. Having chosen likely miRNA candidates from bioinformatics modeling,[10] we chose to further characterize the role of let-7 in MYC transcription factor regulation. Initially, it was thought that to see cleavage of target mRNAs, the complementarity between the target and the miRNA needed to be perfect, a condition that was not met[11] by let-7a and MYC. However, since that report, let-7 has been shown to degrade mRNA in the absence of this stringent complementarity (37), as has been confirmed for other miRNA-mRNA complexes (38). Additionally, several recent articles (39, 40) have shown that this degradation occurs right on the polysomes and not in the RNA-induced silencing complex as had been previously believed. Using 10058-F4 inhibitor to target MYC-MAX transcription factor, time-dependent and end point questions were posed to answer the mechanism and biological consequence of MYC inhibition in initiating the reversal of dysregulated MYC function. In this part of the study, we determined the regulation of MYC mRNA and several miRNAs in comparison with the kinetics of the 10050-F4–induced diminution of the nuclear MYC transcription complex in the Burkitt lymphoma line Namalwa. The temporal analysis of MYC protein, MYC-MAX complex, miRNAs, and MYC mRNA established that significant disruption of the transcription factor complex and increases in several miRNAs occur at ~24 h after inhibitor exposure. Because these molecular events preceded the phenotypic changes in cell growth and subsequent changes in MYC mRNA levels, the results are temporally consistent with the initial up-regulation of let-7a and the subsequent down-regulation of MYC mRNA, as suggested by the transfection experiments (Table 2). We found that the initial decline of MYC-MAX transcription factor activity (3-fold decrease in nuclear MYC protein levels; Fig. 1*A*) and the induction of the miRNAs (Fig. 2*A* and *B*) preceded changes in MYC mRNA and cell growth. Again, a coordinate and inverse regulation of the let-7 family of miRNAs and mir-17-5p followed the MYC transcription factor inhibition. These events were time (Fig. 3*B*) and inhibitor concentration dependent (data not shown). As expected, the disruption of the transcription factor complex resulted in the downstream regulation of MYC transcription factor activity. MYC-activated and MYC-repressed mRNAs were reversed by

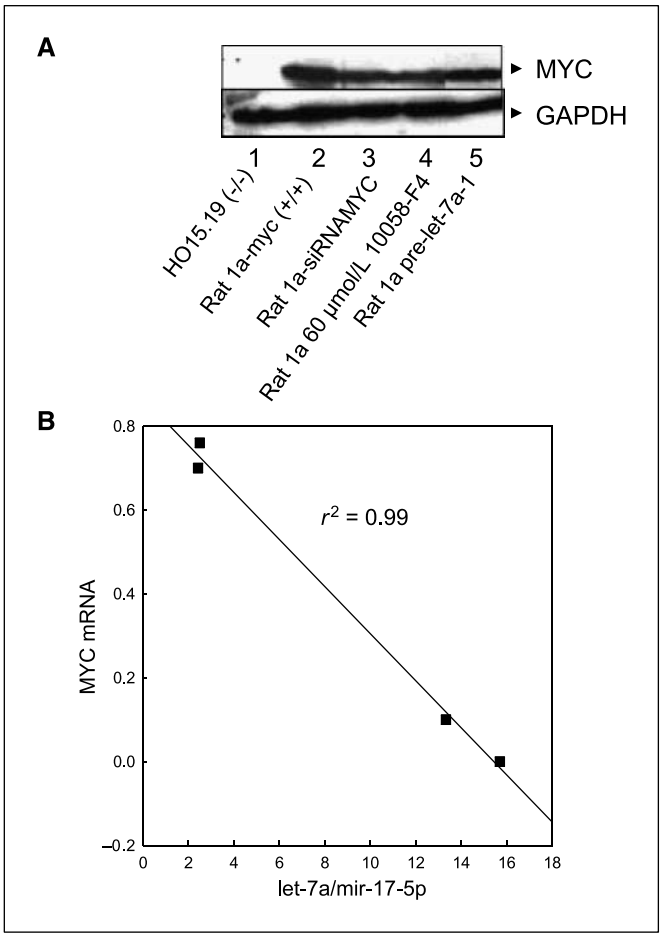

Figure 4. Inhibition of Myc protein and mRNA expression in rat fibroblasts. Myc protein concentrations in transient transfection or inhibitor experiments. *A, top,* immunoblot of Myc in the total cell extract of HO15.19 Myc-knockout cells, rat 1a Myc-transformed cells, and rat 1a Myc-transformed cells transfected with 40 nmol/L pre-let-7a miRNA, 40 nmol/L siRNA Myc, or exposed to 60 μmol/L compound 10058-F4. Myc was detected with anti-MYC antibody (*top*) and glyceraldehyde-3-phosphate dehydrogenase (*GAPDH*) was the loading control (*bottom*). Altered gene expression of Myc mRNA and miRNAs let-7a and mir-17-5p by transfection or inhibition studies. *B,* total RNA extracted from cells treated as described above was assayed by real-time RT-PCR for Myc mRNA and miRNA levels of let-7a and mir-17-5p (see Materials and Methods). The ratio of relative percentage changes in let-7a/mir-17-5p was plotted against the respective Myc mRNA levels for each of the molecules studied (r^2 = 0.99).

[10] http://www.microrna.org
[11] http://microrna.sanger.ac.uk/

transcription factor inhibition, whereas the control mRNAs remained unchanged (Fig. 2*D*). Again, this confirmed the downstream effects of the earlier events.

The Felser laboratory has done extensive modeling of MYC-related tumors in mice (as reviewed in refs. 41, 42) as have several other laboratories (43, 44). Regulation of MYC, even transiently, has resulted in the cessation of tumor growth and the ablation of the residual tumor (45). Although down-regulation of MYC has not always resulted in the eradication of tumor (46, 47), several genetic pathways that augment MYC tumorigenesis have recently been described (48). Gene-specific suppression therapy (e.g., bcl2; ref. 49) or activation therapy (e.g., thrombospondin-1 expression; ref. 50) in these MYC treatment–resistant cancers, however, resulted in tumor ablation and increased survival in most cases. Here we describe a new microcircuitry between MYC mRNA and let-7 and mir-17-5p miRNAs that causes growth arrest in an EBV-associated Burkitt lymphoma line derived from a patient with endogenous Burkitt lymphoma. Whether this is a direct effect of MYC down-regulation itself or a consequence of other downstream altered transcriptional events has yet to be determined. Finally, these results in Burkitt lymphoma and those previously reported for lung (28) and colon (29) cancers validate the apparent regulation of MYC by let-7a and reaffirm its role in the cancer process.

Acknowledgments

Received 7/9/2007; accepted 8/7/2007.

Grant support: NIH grant 2 P20 RR016472-04 and the Nemours Foundation.

The costs of publication of this article were defrayed in part by the payment of page charges. This article must therefore be hereby marked *advertisement* in accordance with 18 U.S.C. Section 1734 solely to indicate this fact.

References

1. Fire A, Xu S, Montgomery MK, Kostas SA, Driver SE, Mello CC. Potent and specific genetic interference by double-stranded RNA in *Caenorhabditis elegans*. Nature 1998;391:806–11.
2. Baehrecke EH. miRNAs: micro managers of programmed cell death. Curr Biol 2003;13:R473–5.
3. He L, Thomson JM, Hemann MT, et al. A microRNA polycistron as a potential human oncogene. Nature 2005;435:828–33.
4. Pfeffer S, Zavolan M, Grasser FA, et al. Identification of virus-encoded microRNAs. Science 2004;304:734–6.
5. Chen CZ, Li L, Lodish HF, Bartel DP. MicroRNAs modulate hematopoietic lineage differentiation. Science 2004;303:83–6.
6. Lee Y, Jeon K, Lee JT, Kim S, Kim VN. MicroRNA maturation: stepwise processing and subcellular localization. EMBO J 2002;21:4663–70.
7. Han J, Lee Y, Yeom KH, Kim YK, Jin H, Kim VN. The Drosha-DGCR8 complex in primary microRNA processing. Genes Dev 2004;18:3016–27.
8. Hutvagner G, Zamore PD. A microRNA in a multiple-turnover RNAi enzyme complex. Science 2002;297:2056–60.
9. Luscher B, Eisenman RN. New light on Myc and Myb. Part II. Myb. Genes Dev 1990;4:2235–41.
10. Persson H, Hennighausen L, Taub R, DeGrado W, Leder P. Antibodies to human c-myc oncogene product: evidence of an evolutionarily conserved protein induced during cell proliferation. Science 1984;225:687–93.
11. Eilers M, Schirm S, Bishop JM. The MYC protein activates transcription of the α-prothymosin gene. EMBO J 1991;10:133–41.
12. Vennstrom B, Sheiness D, Zabielski J, Bishop JM. Isolation and characterization of c-myc, a cellular homolog of the oncogene (v-myc) of avian myelocytomatosis virus strain 29. J Virol 1982;42:773–9.
13. Facchini LM, Penn LZ. The molecular role of Myc in growth and transformation: recent discoveries lead to new insights. FASEB J 1998;12:633–51.
14. Amati B, Littlewood TD, Evan GI, Land H. The c-Myc protein induces cell cycle progression and apoptosis through dimerization with Max. EMBO J 1993;12:5083–7.
15. Grinberg AV, Hu CD, Kerppola TK. Visualization of Myc/Max/Mad family dimers and the competition for dimerization in living cells. Mol Cell Biol 2004;24:4294–308.
16. Pelengaris S, Khan M, Evan GI. Suppression of Myc-induced apoptosis in β cells exposes multiple oncogenic properties of Myc and triggers carcinogenic progression. Cell 2002;109:321–34.
17. Osthus RC, Shim H, Kim S, et al. Deregulation of glucose transporter 1 and glycolytic gene expression by c-Myc. J Biol Chem 2000;275:21797–800.
18. Cole MD, McMahon SB. The Myc oncoprotein: a critical evaluation of transactivation and target gene regulation. Oncogene 1999;18:2916–24.
19. McManus MT. MicroRNAs and cancer. Semin Cancer Biol 2003;13:253–8.
20. Yin X, Giap C, Lazo JS, Prochownik EV. Low molecular weight inhibitors of Myc-Max interaction and function. Oncogene 2003;22:6151–9.
21. Mateyak MK, Obaya AJ, Adachi S, Sedivy JM. Phenotypes of c-Myc-deficient rat fibroblasts isolated by targeted homologous recombination. Cell Growth Differ 1997;8:1039–48.
22. Gomez-Curet I, Perkins RS, Bennett R, Feidler KL, Dunn SP, Krueger LJ. c-Myc inhibition negatively impacts lymphoma growth. J Pediatr Surg 2006;41:207–11.
23. Lawrence JB, Villnave CA, Singer RH. Sensitive, high-resolution chromatin and chromosome mapping *in situ*: presence and orientation of two closely integrated copies of EBV in a lymphoma line. Cell 1988;52:51–61.
24. Hann SR, Eisenman RN. Proteins encoded by the human c-myc oncogene: differential expression in neoplastic cells. Mol Cell Biol 1984;4:2486–97.
25. Basso K, Margolin AA, Stolovitzky G, Klein U, la-Favera R, Califano A. Reverse engineering of regulatory networks in human B cells. Nat Genet 2005;37:382–90.
26. Fernandez PC, Frank SR, Wang L, et al. Genomic targets of the human c-Myc protein. Genes Dev 2003;17:1115–29.
27. O'Donnell KA, Wentzel EA, Zeller KI, Dang CV, Mendell JT. c-Myc-regulated microRNAs modulate E2F1 expression. Nature 2005;435:839–43.
28. Johnson SM, Grosshans H, Shingara J, et al. RAS is regulated by the let-7 microRNA family. Cell 2005;120:635–47.
29. Akao Y, Nakagawa Y, Naoe T. let-7 microRNA functions as a potential growth suppressor in human colon cancer cells. Biol Pharm Bull 2006;29:903–6.
30. Johnston RJ, Jr., Chang S, Etchberger JF, Ortiz CO, Hobert O. MicroRNAs acting in a double-negative feedback loop to control a neuronal cell fate decision. Proc Natl Acad Sci U S A 2005;102:12449–54.
31. Hossain A, Kuo MT, Saunders GF. Mir-17-5p regulates breast cancer cell proliferation by inhibiting translation of AIB1 mRNA. Mol Cell Biol 2006;26:8191–201.
32. Sylvestre Y, De Guire V, Querido E, et al. An E2F/miR-20a autoregulatory feedback loop. J Biol Chem 2007;282:2135–43.
33. Woods K, Thomson JM, Hammond SM. Direct regulation of an oncogenic micro-RNA cluster by E2F transcription factors. J Biol Chem 2007;282:2130–4.
34. Pillai RS, Artus CG, Filipowicz W. Tethering of human Ago proteins to mRNA mimics the miRNA-mediated repression of protein synthesis. RNA 2004;10:1518–25.
35. Valencia-Sanchez MA, Liu J, Hannon GJ, Parker R. Control of translation and mRNA degradation by miRNAs and siRNAs. Genes Dev 2006;20:515–24.
36. Llave C, Xie Z, Kasschau KD, Carrington JC. Cleavage of Scarecrow-like mRNA targets directed by a class of *Arabidopsis* miRNA. Science 2002;297:2053–6.
37. Bagga S, Bracht J, Hunter S, et al. Regulation by let-7 and lin-4 miRNAs results in target mRNA degradation. Cell 2005;122:553–63.
38. Didiano D, Hobert O. Perfect seed pairing is not a generally reliable predictor for miRNA-target interactions. Nat Struct Mol Biol 2006;13:849–51.
39. Maroney PA, Yu Y, Fisher J, Nilsen TW. Evidence that microRNAs are associated with translating messenger RNAs in human cells. Nat Struct Mol Biol 2006;13:1102–7.
40. Kim J, Krichevsky A, Grad Y, et al. Identification of many microRNAs that copurify with polyribosomes in mammalian neurons. Proc Natl Acad Sci U S A 2004;101:360–5.
41. Arvanitis C, Felsher DW. Conditional transgenic models define how MYC initiates and maintains tumorigenesis. Semin Cancer Biol 2006;16:313–7.
42. Shachaf CM, Felsher DW. Tumor dormancy and MYC inactivation: pushing cancer to the brink of normalcy. Cancer Res 2005;65:4471–4.
43. Marinkovic D, Marinkovic T, Mahr B, Hess J, Wirth T. Reversible lymphomagenesis in conditionally c-MYC expressing mice. Int J Cancer 2004;110:336–42.
44. Pelengaris S, Khan M, Evan G. c-MYC: more than just a matter of life and death. Nat Rev Cancer 2002;2:764–76.
45. Jain M, Arvanitis C, Chu K, et al. Sustained loss of a neoplastic phenotype by brief inactivation of MYC. Science 2002;297:102–4.
46. Pelengaris S, Abouna S, Cheung L, Ifandi V, Zervou S, Khan M. Brief inactivation of c-Myc is not sufficient for sustained regression of c-Myc-induced tumours of pancreatic islets and skin epidermis. BMC Biol 2004;2:26.
47. Boxer RB, Jang JW, Sintasath L, Chodosh LA. Lack of sustained regression of c-MYC-induced mammary adenocarcinomas following brief or prolonged MYC inactivation. Cancer Cell 2004;6:577–86.
48. Karlsson A, Giuriato S, Tang F, Fung-Weier J, Levan G, Felsher DW. Genomically complex lymphomas undergo sustained tumor regression upon MYC inactivation unless they acquire novel chromosomal translocations. Blood 2003;101:2797–803.
49. Smythe WR, Mohuiddin I, Ozveran M, Cao XX. Antisense therapy for malignant mesothelioma with oligonucleotides targeting the bcl-xl gene product. J Thorac Cardiovasc Surg 2002;123:1191–8.
50. Giuriato S, Ryeom S, Fan AC, et al. Sustained regression of tumors on MYC inactivation requires p53 or thrombospondin-1 to reverse the angiogenic switch2. Proc Natl Acad Sci U S A 2006;103:16266–71.

MicroRNA Let-7a Down-regulates MYC and Reverts MYC-Induced Growth in Burkitt Lymphoma Cells

Valerie B. Sampson, Nancy H. Rong, Jian Han, et al.

Cancer Res 2007;67:9762-9770.